

The NeuroMedicator—a micropump integrated with silicon microprobes for drug delivery in neural research

S Spieth^{1,4}, A Schumacher¹, C Kallenbach¹, S Messner¹
and R Zengerle^{1,2,3}

¹ Institut für Mikro- und Informationstechnik der Hahn-Schickard-Gesellschaft e.V. (HSG-IMIT), Villingen-Schwenningen, Germany

² Laboratory for MEMS Applications, Department of Microsystems Engineering (IMTEK), University of Freiburg, Freiburg, Germany

³ BIOSS - Centre for Biological Signalling Studies, University of Freiburg, Freiburg, Germany

E-mail: sven.spieth@hsg-imit.de

Received 21 December 2011, in final form 12 March 2012

Published 22 May 2012

Online at stacks.iop.org/JMM/22/065020

Abstract

The *NeuroMedicator* is a micropump integrated with application-specific silicon microprobes aimed for drug delivery in neural research with small animals. The micropump has outer dimensions of $11 \times 15 \times 3 \text{ mm}^3$ and contains 16 reservoirs each having a capacity of $0.25 \mu\text{L}$. Thereby, the reservoirs are interconnected in a pearl-chain-like manner and are connected to two 8 mm long silicon microprobes. Each microprobe has a cross-sectional area of $250 \times 250 \mu\text{m}^2$ and features an integrated drug delivery channel of $50 \times 50 \mu\text{m}^2$ with an outlet of $25 \mu\text{m}$ in diameter. The drug is loaded to the micropump prior to implantation. After implantation, individual $0.25 \mu\text{L}$ portions of drug can be sequentially released by short heating pulses applied to a polydimethylsiloxane (PDMS) layer containing Expance1[®] microspheres. Due to local, irreversible thermal expansion of the elastic composite material, the drug is displaced from the reservoirs and released through the microprobe outlet directly to the neural tissue. While implanted, leakage of drug by diffusion occurs due to the open microprobe outlets. The maximum leakage within the first three days after implantation is calculated to be equivalent to $0.06 \mu\text{L}$ of drug solution.

(Some figures may appear in colour only in the online journal)

1. Introduction

Drug delivery to neural tissue is very important in the treatment of brain-related diseases. There are different administration routes to provide drugs to neural tissue, e.g. by oral administration or injections into the bloodstream. However, certain drugs are rejected by the blood–brain barrier that protects the brain or need to be administered fast and highly localized into a specific brain region. In this case, invasive neural drug delivery by microprobes is considered to be one of the most promising methods since the liquid drug can be directly delivered into a specific brain region.

Two invasive research methods to introduce minute amounts of drugs are distinguished in neuroscience: microiontophoresis and pressure ejection [1, 2]. Microiontophoresis allows the injection of charged drug compounds from a drug solution by electrical currents. Consequently, this method is not suitable for drugs with low charge-to-mass ratios. Additionally, it is impossible to determine accurately the amount of injected drug from the applied current. Pressure ejection, i.e. pressure-driven liquid infusion, is independent of the charge states of the drug molecules. However, diffusion-based leakage of drug from the microprobe, channel blockages and physical displacement of the surrounding tissue during injection are typically of concern. Apart from the mentioned

⁴ Author to whom any correspondence should be addressed.

drawbacks, liquid infusion is considered to be the more versatile drug delivery method.

Previously, different fluidic microprobes for neural research have been presented by micromachining of various materials. Microprobes made of silicon have been described by several researchers [3–9]. Furthermore, microprobes made from other materials such as glass [10], parylene [11–13], polyimide [14] and SU-8 [15] have also been presented. However, whereas chronically implanted silicon-based microprobes containing electrodes for recording and stimulation are meanwhile already used in humans [16], multifunctional probes offering additionally integrated drug delivery are still under development and are mostly limited to acute applications [17, 18]. This is a consequence of the increased complexity of integration of a microfluidic probe assembly in comparison to a pure electrode system. Electrodes can easily be connected to electric micro connectors to achieve a highly miniaturized, pluggable, chronic system. However, there is no pluggable and self-sealing microfluidic connector compatible with volume deliveries on the order of submicrolitres. Moreover, a pluggable connector can introduce contamination into the microfluidic system possibly causing infections. Consequently, a permanent fluidic connection of the microprobes either to a macroscopic pump or a miniaturized drug delivery system which can be placed directly next to the probes is required. Considering mobility aspects, especially in small animal research, a miniaturized system is definitely more desirable. In addition, the reduced complexity of an electric device interface in comparison to a fluidic connection enables the perspective of stand-alone operation as well as wireless controllability. However, only a few miniature drug delivery systems with attached microprobes for liquid infusion directly into neural tissue have been proposed. For instance, early approaches applied electrolysis directly in the drug solution to generate the flow needed for infusion thereby accepting possible degradation of the drug [19, 20]. Furthermore, a mechanical pump with microprobes has been presented [21] and commercially available general-purpose drug delivery pumps not specifically tailored for microprobes can be modified to realize brain infusions [22, 23]. Both electrolysis-based as well as mechanical pumps allow for electric control and can be regarded as ‘drug-on-demand’ systems. On the other hand, osmotic capsules with connected brain infusion sets are commercially available [24] and offer constant drug delivery, but without the option of controllability.

The ideal drug delivery system used for experimental studies in neural research with animals should feature multifunctional microprobes, be small in size, designed for single use to prevent cross-contamination between experiments, able to store the liquid drug within the system, and enable the release of a specified number of liquid infusions through the microprobes into the neural tissue. Additionally, the system should not alter the drug during operation. A significant reduction in system complexity can be achieved by restriction to the delivery of well-defined discrete liquid volumes instead of enabling any variable volume. The complexity is further reduced when the volume of drug to be delivered equals directly the quantity stored in an individual

reservoir, possibly being part of a whole array of reservoirs within the implant.

A single-use drug-on-demand system ideally contains an irreversible or bistable actuation mechanism that offers high volume displacement and which can be electrically initiated. Most actuators which fulfil these criteria are based on changes in material composition or involve gases. For instance, one-way shape memory alloys [25] and polymers [26] can recover to predefined shapes thereby displacing well-defined volumes. Even higher volume displacements can be realized by using gas-based actuators which take advantage of the large expansion capabilities of gases. Typically, the involved gases result from phase transitions [27] or are generated by substance decomposition during electrolysis [28, 29], thermolysis [30–32], micropyrotechnics [33, 34] or catalytic reactions [35, 36]. Additionally, pressurized gases can be released upon request and used as propellant [37]. However, equilibrium reactions such as electrolysis tend to be not completely stable and temperature dependent phase transitions require typically additional mechanical means to maintain stable position at varying temperature [27]. In general, one critical issue of gas and phase transition-based actuation mechanisms is the encapsulation of the gas phase. In particular, if elastic elements such as membranes are employed, gas permeability becomes a major concern. In the case of polymers, high stretchability is associated with weak crosslinking of the molecular chains [38]. In turn, this promotes gas permeability. Gas leakage can reduce the lifetime or even cause complete malfunction of a gas-based actuator.

Thermally expandable microspheres have been introduced by the Stemme group as an actuation material in microfluidics [39–43] and belong to the phase transition-based actuators. These so-called Expancel[®] (Expancel, Sundsvall, Sweden) are polymeric shells of about 10 μm in diameter containing a liquid hydrocarbon. As the hydrocarbon is normally volatile at room temperature, it is stored above its vapour pressure inside the shells. Heating above a critical temperature softens the polymeric shell and allows the vapour pressure to relax leading to a volumetric expansion by a factor of up to 60. When heating is switched off, the polymeric shell solidifies and prevents shrinkage making the expansion irreversible. The microspheres can be mixed with liquid polydimethylsiloxane (PDMS) and consequently be as easily processed [41]. Since each microsphere acts as an individual actuator by itself, extreme redundancy together with uncritical handling is available. Additionally, it has been demonstrated that this type of actuator can create sufficiently high displacements as well as pressures at a reasonably low temperature load on the liquid in microfluidics [39, 41–43].

We applied the Expancel[®]–PDMS composite material to develop the prototype of the *NeuroMedicator* [44], a small-scale drug-on-demand system designed for use in neuroscience research with small animals such as rats. The *NeuroMedicator* combines a micropump with silicon fluidic microprobes developed within the EU-funded *NeuroProbes* project [45, 46]. Predefined portions of drug can be released by local heating of the composite material which displaces the liquid drug from an array of well-defined reservoirs.

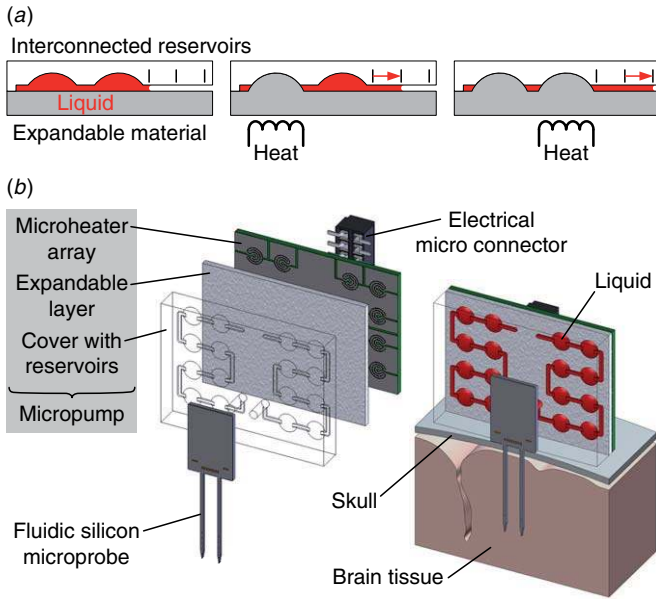


Figure 1. (a) Illustration of the micropumping principle of the *NeuroMedicator*. (b) Exploded view of the technological implementation of the *NeuroMedicator* and placement on the skull.

2. Materials and methods

2.1. Principle of operation

The principle and technological implementation of the *NeuroMedicator* is illustrated in figure 1. A fluidic silicon microprobe is connected to liquid reservoirs which are arranged in a pearl-chain-like arrangement with a blind end. Prior to implantation, the liquid reservoirs are filled with drug through the silicon microprobes (figure 1(a)). For this purpose, the whole device is placed into a vacuum desiccator to remove any air within the device. Once the vacuum is established, the microprobes are partially immersed into liquid drug. Balancing the desiccator again with atmosphere pushes the liquid through the microprobes into the evacuated reservoirs. Before implantation, any remaining liquid on the outside of the microprobes is removed, e.g. by using alcohol. After implantation of the probes, sequential heating of the Expancel®-PDMS composite material underneath the liquid reservoirs displaces the liquid stored in the reservoirs as shown in figure 1(a). Since the expansion of the material is irreversible, no backflow occurs. Hence, each actuation cycle pumps precisely the liquid volumes predefined by the reservoirs through the silicon microprobes without the need for additional sensor control.

The technological implementation of the *NeuroMedicator* is illustrated in figure 1(b). The device consists of a micropump with an attached electrical micro connector and fluidic silicon microprobes. The micropump is based on three different components: (i) a substrate with an individually addressable microheater array, (ii) a thermally expandable layer with Expancel® embedded into a PDMS matrix and (iii) a cover containing interconnected reservoirs for liquid storage. Each of the two microprobe shafts is fluidically connected to eight liquid reservoirs of 0.25 μL in a pearl-chain-like arrangement.

When the device is mounted on the skull of the subject, the microprobe shafts penetrate into the brain region of interest. After electrical connection, well-defined liquid drug portions can be infused via the two microprobes into the tissue by remote control.

2.2. Drug leakage by diffusion

A general concern of pressure-driven liquid infusion in neuroscience is the unintended leakage of drug from the probe outlet by diffusion. The *NeuroMedicator* is designed as a semi-chronic device for short time use. While implanted, the probe outlets are directly connected to the drug reservoirs. Consequently, the concentration gradient will result in a diffusion flux from the reservoirs via the outlets into the brain. While some groups take advantage of this phenomenon for diffusion-driven drug delivery [5], others try to avoid diffusion by integration of microvalves directly at the outlets of the microprobes [7]. However, due to the severe size constraints for such elements, only passive mechanical shutters which seal the outlets have been realized on neural probe shafts so far. It was demonstrated *in vitro* that unintended diffusion could be reduced by a factor of about 25 [7], but it is not clear if this performance is also maintained after *in vivo* implantation. The cellular environment could affect the proper operation of the shutters making them less effective. Approaches to integrate active elements, such as thermopneumatic valves [7], have been limited to the probe backbone. Consequently, this cannot completely prevent the diffusion of the drug remaining in the channel section between outlet and valve in the probe shaft. In our application, the amount of drug stored in the probe channel is small compared to the intended infusion volume. In that case, the long and narrow fluidic channels significantly slow down the diffusion and reduce the drug leakage to a tolerable level. This will be quantified in the next section.

The fluidic silicon microprobes used for the *NeuroMedicator* comprise two 8 mm long shafts with a cross-sectional area of $250 \times 250 \mu\text{m}^2$ attached to a common platform of $6 \times 4 \text{ mm}^2$ as shown in figure 2(a). The diameter of a fluidic inlet port is 300 μm , whereas the diameter of the outlet ports is 25 μm . Both ports are oriented out-of-plane on opposite sides of the probe. The 9.5 mm long microfluidic channel narrows from a cross-section of $300 \times 50 \mu\text{m}^2$ at the inlet to $50 \times 50 \mu\text{m}^2$ in the probe shaft. A more detailed description of the probe geometries is provided in [9]. To estimate the leakage of drug, we applied the multiphysics simulations software CFD-ACE+ (CFD Research Corporation, Huntsville, AL, USA). The boundary conditions were chosen to approximate the initial case where a fluidic microprobe is completely primed with drug solution and afterwards inserted into the brain with no further action undertaken. Three-dimensional transient diffusion processes of species in liquids can be described by Fick's second law of diffusion:

$$D\nabla^2 c = \frac{\partial c}{\partial t} \quad (1)$$

where c is the species concentration, t the time, and D the temperature-dependent diffusion coefficient which describes

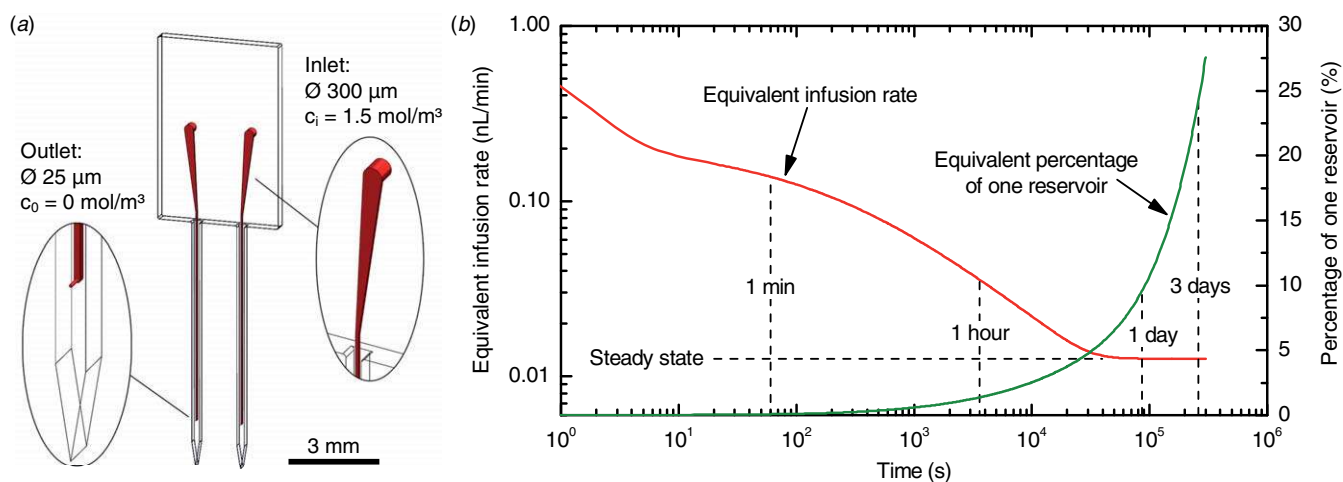


Figure 2. CFD-simulation of the diffusion-based leakage from the probe outlet. (a) Microprobe geometry. (b) Leakage rate expressed as an equivalent infusion rate and total drug amount lost over time expressed as percentage of the amount stored in a $0.25 \mu\text{L}$ reservoir.

the mobility of the species. The *NeuroMedicator* is designed to provide drug solution on demand, e.g. an agonist mixture of muscimol and baclofen for temporary inactivation of a certain brain region. Typical diffusion coefficients of neurotransmitters for diffusion in solutions are on the order of 6.6×10^{-6} to $7.5 \times 10^{-6} \text{ cm}^2 \text{ s}^{-1}$ at 37°C as summarized by Rice *et al* [47]. Therefore, a representative diffusion coefficient of $D = 7 \times 10^{-6} \text{ cm}^2 \text{ s}^{-1}$ was assumed for the simulation. Although a drug concentration of $c_i = 1.5 \text{ mol m}^{-3}$ was applied to the numerical calculation, all results are stated in a normalized form making them valid for any initial concentration c_i having a similar D .

The simulation was performed for a worst-case scenario. The drug concentration at the silicon probe inlet c_i is assumed to be constant and the brain is modelled as an ideal sink with concentration $c_0 = 0 \text{ mol m}^{-3}$. In reality, the surrounding tissue at the probe outlet becomes enriched with drug and the drug liquid next to the probe inlet becomes depleted which reduces the concentration gradient and in turn the diffusion flux. Additionally, it has to be noted that diffusivity in brain tissue can be more than one order smaller than in solution [47].

The diffusion-based leakage rate expressed as an equivalent infusion rate as well as the total drug amount lost over time expressed as a percentage of the total amount stored in a $0.25 \mu\text{L}$ reservoir are shown in figure 2(b). For our target application, the maximum time interval between consecutive drug delivery experiments is estimated to be around 3 days. During this time, drug corresponding to $0.06 \mu\text{L}$ drug solution, being equivalent to 24% of the amount stored in one reservoir, is released by diffusion-based leakage. However, considering the applied worst-case conditions and the very low release equivalent to an infusion rate of less than 1 nL min^{-1} , the diffusive drug release should stay well below the level which would cause a reaction.

The liquid volume inside the microprobe is only $0.06 \mu\text{L}$ and equals 24% of a $0.25 \mu\text{L}$ drug portion stored in one of the reservoirs (which corresponds by chance to the previously determined amount of drug leaked by diffusion). Therefore, the diffusion-based leakage results in depletion of the drug stored inside the interconnected reservoirs. A whole

actuation sequence includes eight infusions of $0.25 \mu\text{L}$ at times $t = 3, 6, \dots, 24$ days after implantation. Given the assumption that the boundary conditions at the microprobe c_i and c_0 are constant during the three day intervals and the concentration gradient along the interconnected reservoirs in the cover is negligible, the drug depletion can be estimated by using a model calculation not further detailed here. According to this calculation, the drug concentration of the first infusion is reduced by 7%, whereas the last infusion is reduced by 21% with respect to the original concentration. Therefore, depletion of the stored drug liquid might have to be considered in the case of long implantation times, keeping in mind that these estimates are based on a worst-case scenario.

2.3. Substrate materials for microheaters

An individually addressable array of microheaters is required for the local heating of the Expancel[®]-PDMS composite above the critical temperature for expansion. Among the available Expancel[®] grades, Expancel 820 DU 40 offers the lowest expansion temperature which starts at $76\text{--}81^\circ\text{C}$ [48]. The Stemme group which introduced the microspheres to the MEMS community fabricated microheaters by photolithographical patterning of copperclad laminates made from glass-reinforced epoxy (FR-4) [40–43]. This choice was mainly based on the fact that FR-4 is a low-cost standard material rather than it would be the best material in terms of power consumption. In the case of the *NeuroMedicator*, the total power consumption of the system has to be minimized and the heat energy has to be concentrated in the Expancel[®]-PDMS composite to prevent temperature increase of the drug.

Typically, placement of microheaters onto thin membranes allows advantage to be taken of the excellent thermal isolation properties of air thereby minimizing heat losses into the substrate. However, in the present case the substrate must be still stiff enough to mechanically enforce the expansion process toward the drug displacement. Any deformation or rupture of the heater area during expansion will decrease the efficiency of the volume displacement used for actuation or even cause malfunction. Therefore, the bulk

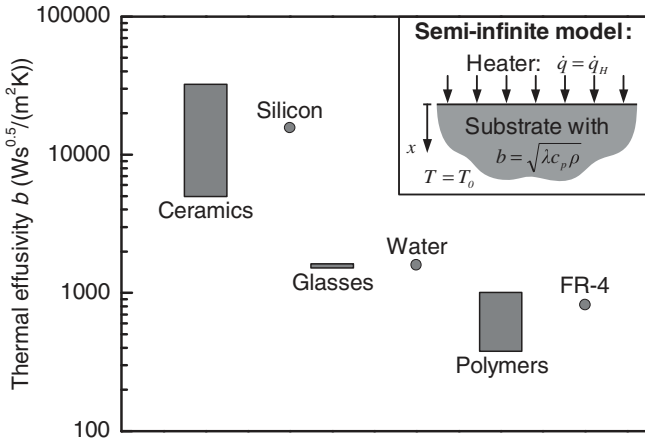


Figure 3. Spectra of the thermal effusivities b of different material classes according to a semi-infinite substrate model subject to a constant heat flux \dot{q}_H from the heater.

material property of the substrate becomes important. Finally, an individually addressable array of N microheaters requires $N+1$ electrical connections which have to be connected to an electric interface. Therefore, it is desirable to be able to use multiple substrate layers for electrical wiring as well as interface implementation to maximize the array density.

The suitability of substrate materials for microheaters can be evaluated by considering the simplified model of a semi-infinite substrate of uniform initial temperature $T = T_0$ which is subject to a constant heat flux boundary condition $\dot{q} = \dot{q}_H$ at $x = 0$ as shown in figure 3. Neglecting other losses, \dot{q}_H represents the heat flux from the dissipated electrical power P of the microheater. In this case, the transient heat distribution is described by the one-dimensional heat equation [49, 50]:

$$a \frac{\partial^2 T}{\partial x^2} = \frac{\partial T}{\partial t} \quad \text{where} \quad a = \frac{\lambda}{\rho c_p} \quad (2)$$

with the spatial coordinate x , temperature T and thermal diffusivity a composed of thermal conductivity λ , density ρ and specific heat capacity c_p .

For the given boundary conditions, an analytical solution for the transient temperature distribution exists [49, 50]:

$$T(x, t) = T_0 + \frac{\dot{q}_H}{\lambda} \left[2\sqrt{\frac{at}{\pi}} \exp\left(-\frac{x^2}{4at}\right) - x \left(1 - \operatorname{erf}\left(\frac{x}{2\sqrt{at}}\right) \right) \right]. \quad (3)$$

The temperature on the surface can be calculated for $x = 0$ which results in

$$T(x = 0, t) = T_0 + \frac{\dot{q}_H}{b} \frac{2}{\sqrt{\pi}} \sqrt{t} \quad \text{with} \quad b = \sqrt{\lambda c_p \rho} \quad (4)$$

where b is the thermal effusivity of a material which represents its ability to exchange thermal energy [49]. It should be noted that λ , c_p and ρ contribute equally to this material property. Consequently, in order to achieve maximum heater temperature with minimum power requirement, the thermal effusivity b needs to be minimized. The thermal effusivity spectra of popular material classes used in MEMS technology are shown in figure 3. Thereby, b decreases from

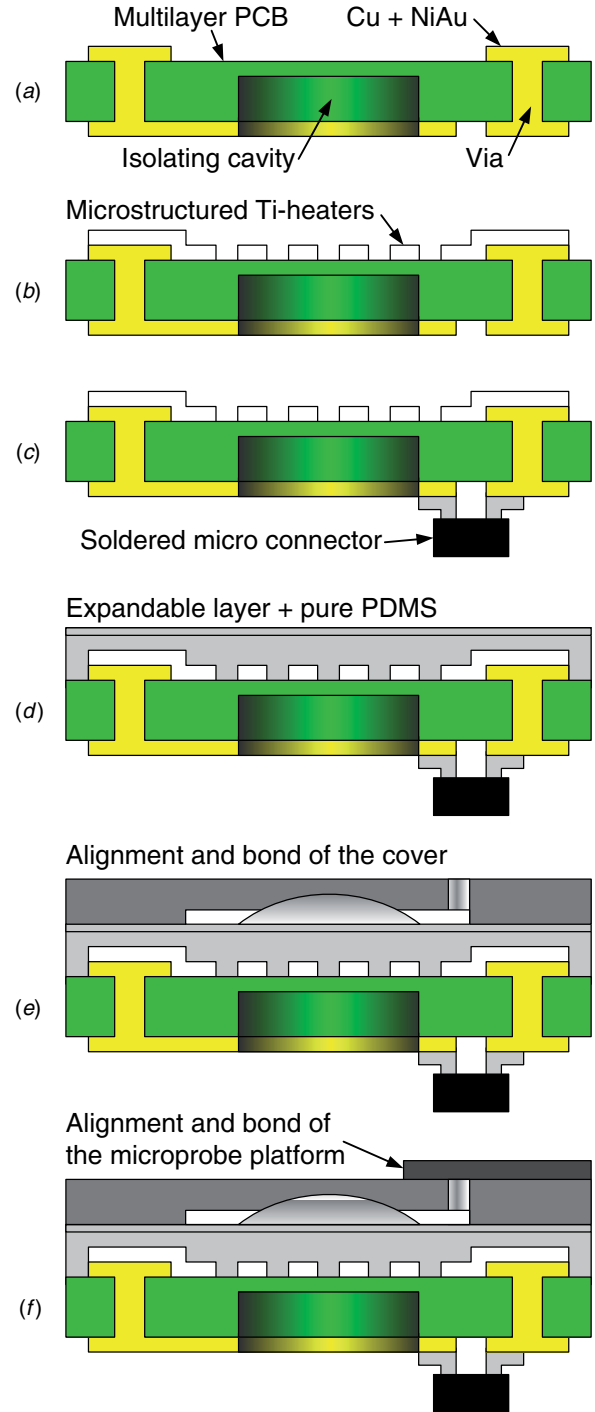


Figure 4. Schematic illustration of the fabrication and the assembly of the different components of the *NeuroMedicator*.

ceramics over glasses to polymers. FR-4, a composite material typically used for printed circuit boards (PCBs), offers a reasonable compromise between a low b as well as established technologies to realize electric multilayers and vias. Therefore, FR-4 is considered to be a suitable substrate material and is used in the following.

2.4. Design, fabrication and assembly

The complete fabrication and assembly sequence of the *NeuroMedicator* is schematically shown in figure 4.

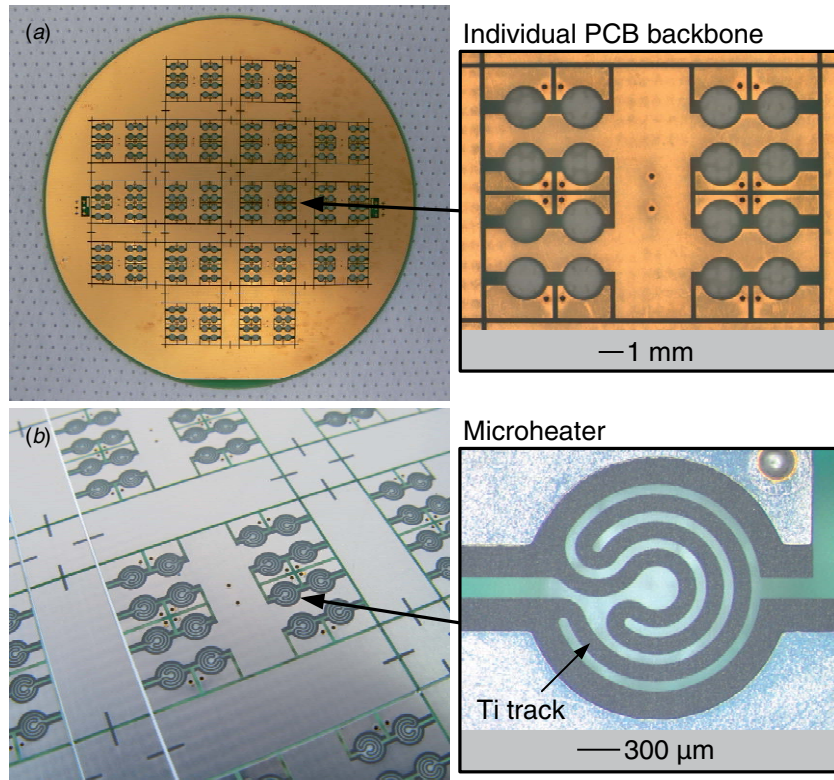


Figure 5. Thin film fabrication of the microheaters. (a) Multilayer PCB 100 mm disc. (b) Fabricated microheaters after deposition and etching of Ti.

Thereby, the microstructured PCB, the cover containing the interconnected reservoirs and the fluidic silicon microprobes are first fabricated as individual components. The following subsections describe the fabrication of the components followed by the assembly sequence of the entire device.

2.4.1. Microstructured PCBs as heater arrays. The heater array was fabricated in PCB technology using custom-made FR-4 substrates (ANDUS Electronic, Berlin, Germany) as shown in figure 4(a). Whereas the μm thick copper (Cu) layers of standard copperclad laminates used in PCB technology together with the high electrical conductivity of Cu are desirable for electrical connections, using them for fabrication of Cu-microheaters is not beneficial. Since the layer thickness cannot be changed and the minimally achievable structure width is technologically limited, this would result in very low-ohmic heaters which require currents of a few hundred milliamperes at voltages far below 1 V during operation. This can complicate stand-alone operation when power is only available from 3 V button cells. Therefore, the microheater itself was fabricated from a different material with lower thickness and higher resistance. To ensure good electric contact to the heater material, oxidation of the underlying Cu is prevented by galvanic deposition of nickel gold (NiAu). Additionally, the FR-4 material was selectively thinned to a thickness of $150\ \mu\text{m}$ underneath the microheaters for better thermal isolation (figure 4(a)).

To facilitate lithographic processing, the PCBs have been designed as 100 mm disks. Each disk is about $500\ \mu\text{m}$ thick and contains 16 *NeuroMedicator* backbones of $11 \times 14.5\ \text{mm}^2$.

After PCB fabrication, the microheaters are realized by sputter deposition of titanium (Ti) on top of the substrates and subsequent thin-film processing (figure 4(b)). A bare PCB disc and the microstructured Ti heaters are shown in figures 5(a) and (b), respectively. The Ti tracks of the heaters have a width of $150\ \mu\text{m}$ and a thickness of $400\ \text{nm}$. After thin-film processing, dicing of the backbones is performed on a standard wafer saw.

2.4.2. Cover containing the interconnected reservoirs. The cover containing the reservoirs is fabricated by replica moulding of biocompatible PDMS RTV615 having a hardness of 44 Shore A (Momentive Performance Materials, Inc., Albany, NY, USA). To ensure complete depletion of the reservoirs after actuation, the $0.25\ \mu\text{L}$ reservoirs are designed as spherical caps which are connected by $300 \times 150\ \mu\text{m}^2$ channels. For similar PDMS types, a two-dimensional shrinkage of 1.5% after thermal cure at $80\ ^\circ\text{C}$ was reported [51]. Therefore, this has already been accounted for in the design process. The three-step fabrication process with corresponding scanning electron microscopy (SEM) micrographs is illustrated in figure 6. First, a positive master of the microfluidic structure comprising reservoirs and channels is milled into poly(methyl methacrylate) (PMMA) as shown in figure 6(a). Thereby, the shape of the spherical caps is determined by standard ball nose cutters. Afterwards, a negative mould is cast with epoxy (SpeciFix-20, Struers GmbH, Willich, Germany) (figure 6(b)). The 2 mm thick cover is then created by PDMS replica moulding and cured at $80\ ^\circ\text{C}$

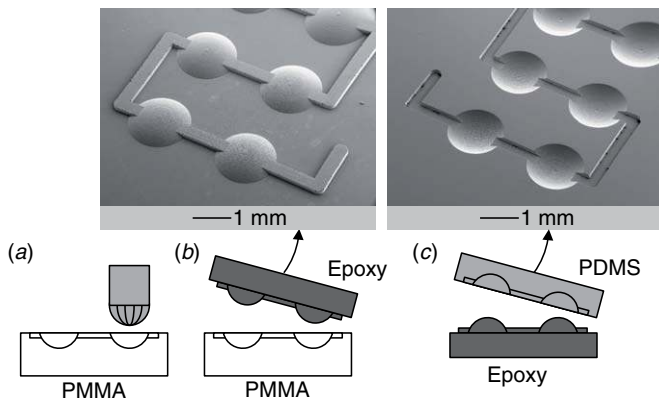


Figure 6. Three-step fabrication process of the cover containing the interconnected reservoirs: (a) Milling of a positive PMMA master, (b) casting of a negative epoxy mould, and (c) PDMS replica moulding of the cover.

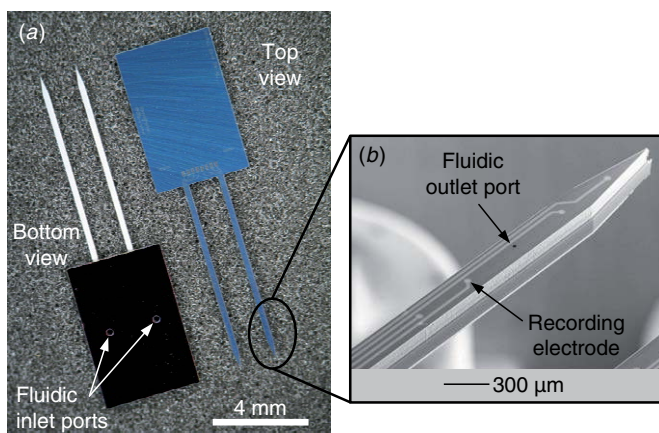


Figure 7. Fabricated fluidic silicon microprobes. (a) Top and bottom views of the microprobes. (b) SEM picture of the probe tip with outlet port and recording electrodes.

(figure 6(c)). Finally, through holes with a diameter of 700 μm are punched-out by using a sharpened steel capillary.

2.4.3. Fluidic silicon microprobes. The fluidic silicon microprobes described previously are fabricated in a two-wafer silicon fusion bond process applying standard 300 μm thick 4 inch silicon (1 0 0) wafers, deep reactive ion etching (DRIE), wafer grinding and thin film processing [9]. The fabricated probes are shown in figure 7. Electrodes on the probe shafts allow for future electrophysiological recordings parallel to drug delivery (figure 7(b)). Previously, similar microprobes based on the same fabrication technologies were verified in *in vivo* experiments to be highly biocompatible [52].

2.4.4. NeuroMedicator assembly. After fabrication of the PCBs (figure 4(a) and microheaters (figure 4(b)), an electrical micro connector (CLM Series, Samtec Europe GmbH, Germering, Germany) is first attached to an individual PCB backbone by reflow soldering (figure 4(c)). To promote adhesion of the subsequent layers, an adhesion promoter is applied to the microstructured surface of the PCB. The expandable material is prepared by mixing PDMS RTV615 (Momentive Performance Materials, Inc., Albany, NY, USA)

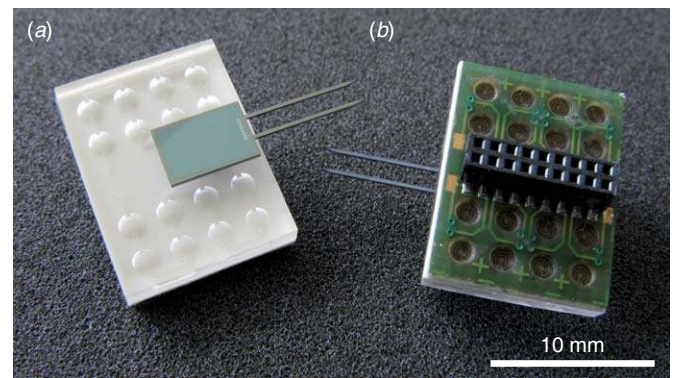


Figure 8. Assembled *NeuroMedicators* showing (a) the top side with the liquid reservoirs and the microprobes as well as (b) the bottom side with the electrical micro connector.

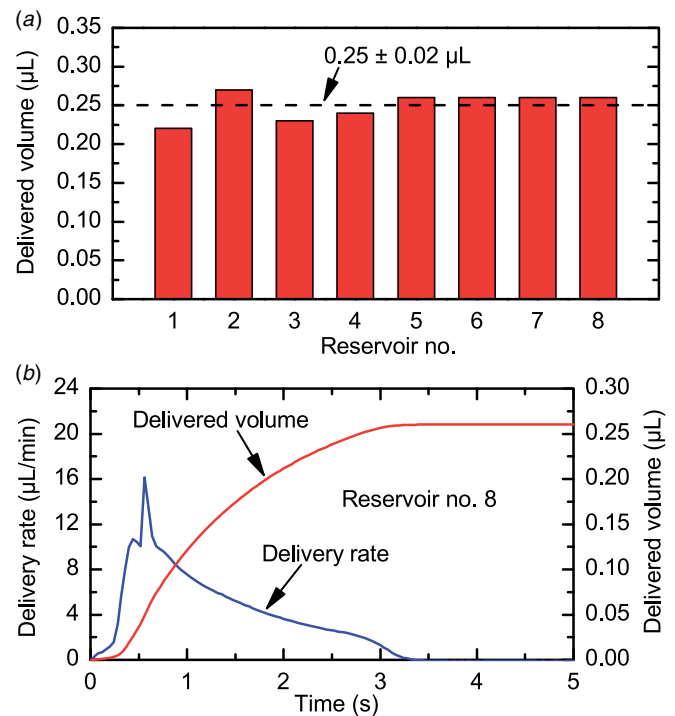


Figure 9. Representative delivery characteristic of a micropump after individual heating with 225 mW for 10 s. (a) Delivered liquid volumes in consecutive order for one half of the device. (b) Transient delivery rate and delivered volume for reservoir no. 8.

with Expancel 820 DU 40 (Expancel, Sundsvall, Sweden) at a weight ratio of 2:1. A 500 μm thick expandable layer is spincoated on the top side of the PCB using a custom-made chuck and cured at moderate 60 °C to prevent early expansion of the microspheres (figure 4(d)). An additional 100 μm thick layer of pure PDMS separates liquids from the expandable material and promotes subsequent bonding of the cover. Then, the cover with the reservoirs is oxygen plasma bonded onto the expandable material (figure 4(e)). Since the liquid reservoirs have to be situated directly above the heating elements which are now not visible anymore, a double-sided alignment is required. This is realized on a modified flip-chip bonder (FINEPLACER® pico, Finetech GmbH & Co. KG, Berlin, Germany). At this point, the fabrication of the micropump is finished. For fabrication of the *NeuroMedicator*, the platform

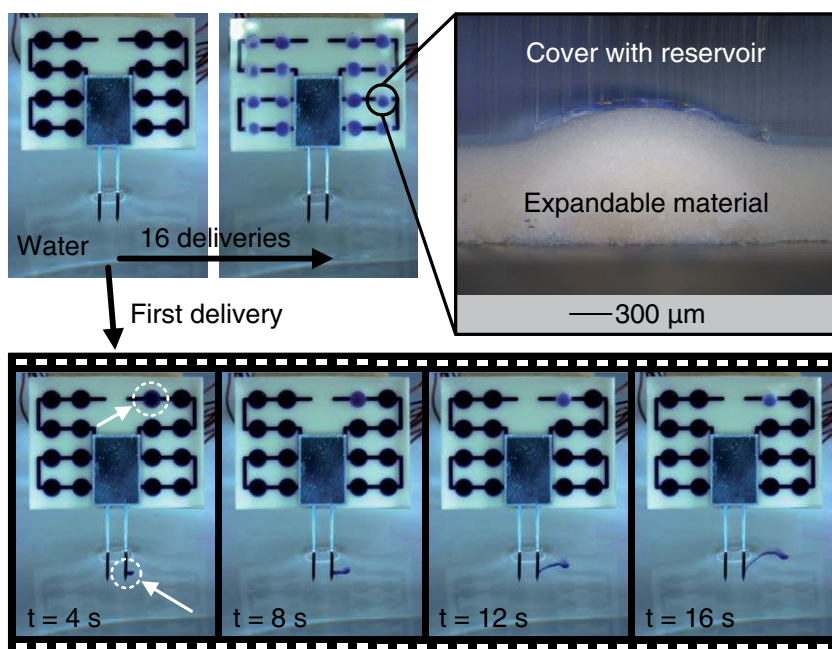


Figure 10. Transient actuation of an ink-filled *NeuroMedicator* with the probe tips inserted into water. A cross section of an actuated reservoir shows complete delivery.

of the fluidic microprobes is additionally bonded on top of the microfluidic structure by using oxygen plasma (figure 4(f)). Since the fluidic inlet ports of the microprobe platform have to match exactly the through-holes of the cover, face-to-face alignment on a flip-chip bonder is required. Top and bottom of assembled *NeuroMedicators* are shown in figure 8.

3. Experimental results

The average resistance of 112 Ti microheaters on 7 micropumps was determined to be $586 \pm 76 \Omega$. Since the resistance is increasing with temperature and might vary slightly from device to device, power-controlled heating was implemented. A programmable source meter (Model 2602, Keithley Instruments, Inc., Cleveland, OH, USA) was used to maintain the heating power on a level of 225 mW during the whole actuation time of typically 10–20 s to activate the composite material.

First, a micropump without microprobes was characterized. For this purpose, fluidic tubing with an inner diameter of $400 \mu\text{m}$ was inserted into the through-holes of the cover. After filling the device with water, the delivered liquid volumes (figure 9(a)) as well as the transient delivery characteristics (figure 9(b)) of the micropump were characterized with a microbalance (LE26P, Sartorius AG, Göttingen, Germany) and a thermal flow sensor (HSG-IMIT, Villingen-Schwenningen, Germany), respectively. Individual heating with 225 mW for 10 s resulted in an average delivered volume of $0.25 \pm 0.02 \mu\text{L}$ for eight consecutive deliveries. The transient characteristics show a steep increase in delivery rate within half a second followed by a slow descent. All of the liquid is delivered within 3 s.

After that, operation of the fully assembled *NeuroMedicator* was optically verified by filling the reservoirs through

the microprobes with concentrated ink and sequential delivery into water as shown in figure 10. To achieve complete delivery and to prevent liquid backflow into the reservoir, the heating time had to be doubled to 20 s. This can be attributed to the increased flow resistance of the microprobe in comparison to the tubing used for characterization of the micropump. Although certain parts of the reservoirs remained stained due to the highly concentrated ink, cross sections of actuated reservoirs prove complete displacement of the reservoir volume by the composite material.

During heating, the critical temperature for expansion of the microspheres is first reached close to the microheater. In this phase, most of the reservoir content is already displaced as shown in figure 9(b). In fact, SEM images of actuated reservoirs revealed that the embedded microspheres close to the liquid reservoir are not expanded. This confirms that there is no significant heat load on the liquid during displacement.

The use of the Expancel[®]-PDMS composite material for actuation and PDMS for the cover offers the convenience of easy handling, replication and bonding. However, PDMS is also known as a material with high vapor permeability and liquid absorption. Encapsulating the device with a barrier material such as parylene-C reduces evaporation, but does not affect liquid absorption inside the PDMS. Consequently, the liquid content of the reservoirs vanishes over time. This limits the liquid storage stability for the current configuration to approximately 24 h at ambient conditions.

4. Conclusions

The *NeuroMedicator* is a prototype of a novel compact drug delivery system for semi-chronic use in the neurosciences. Its proper operation could be successfully demonstrated. In

the configuration presented here, it enables the precise on-demand infusion of 16 discrete $0.25 \mu\text{L}$ portions of liquid drug through 8 mm long silicon microprobes. The device has to be filled once prior to implantation and the microprobes remain implanted over the whole time of operation.

Since unintended leakage of drug by diffusion from the microprobes is of concern, drug diffusion was numerically simulated by using Fick's laws. The long and narrow fluidic channels in the microprobes have a total volume of only $0.06 \mu\text{L}$ and limit the diffusion-based leakage. For worst-case conditions, drug equivalent to $0.06 \mu\text{L}$ drug solution is lost by diffusion after 3 days of implantation. This corresponds to 24% of a $0.25 \mu\text{L}$ drug portion that is typically delivered within less than 1 minute when the *NeuroMedicator* is activated. The associated decrease in drug concentration within the reservoirs can be tolerated. With every portion of drug delivered by the system, drug solution is displaced from a given reservoir to its proximal neighbour. This way, diluted drug from the proximal end of the *NeuroMedicator* is delivered into the brain and replaced by higher concentrated drug from the distal reservoirs. The depletion can be slowed down either by further reducing diffusion from the microprobe or by enlarging the liquid volume stored in the device. To reduce diffusion from the microprobe, a very long and narrow fluidic channel is required, increasing the fluidic resistance and the required pressure during infusion at the same time. On the other hand, a larger liquid volume results in a lower percentage of depletion. However, if number or volume of the liquid reservoirs may not be changed, only the dead volumes (e.g. cross sections of the microfluidic channels connecting the individual reservoirs, etc) can be enlarged, which is generally not desirable. For the given design, the dead volume corresponds to 45% of the overall liquid stored in the device. It should be noted that the Fickian approach does not yet account for possible interactions between different diffusing species. Moreover, species which might diffuse into the device are not considered.

The micropump integrated within the *NeuroMedicator* takes advantage of the local, irreversible thermal expansion of microspheres embedded into PDMS. Therefore, a microheater array serves as the backbone of the micropump. FR-4 was identified as the most promising substrate material with respect to energy efficiency as well as functional aspects such as the possibility for electrical vias. To minimize power consumption, PCB technology was combined with MEMS thin film technology. The power requirement of 225 mW can be regarded to be very good with respect to similar thermally operated devices published by others [40, 43]. The total energy consumption for delivering a single drug portion through the silicon microprobes is 4.5 W.

Standard milling with ball nose cutters in combination with a three-step replica moulding process allows simple fabrication of spherical caps in fluidic PDMS structures. Additionally, volume and space consumption of the liquid reservoirs can be easily adapted to the delivery requirements. The spherical shape allows the expanding material to completely displace the reservoir volume since no sharp edges exist. However, for a given cutter diameter the volume of a spherical cap is related to the milling depth by a cubic

polynomial. Therefore, very precise adjustment of the milling depth during fabrication is required. Furthermore, a shrinkage of 1.5% for curing at 80°C has to be considered for PDMS to achieve precise reservoir volumes.

The micropump proved to be able to precisely deliver liquid portions of $0.25 \pm 0.02 \mu\text{L}$. However, experiments also showed that the fluidic resistance of the microprobes in conjunction with the observed delivery rate doubles the actuation time needed from 10 s to 20 s. Hence, slower heating rates resulting in smaller delivery rates and smaller transient pressure gradients would be preferable. For instance, this can be achieved by a sequence of shorter and lower heat pulses rather than continuous heating.

The limited long-term stability can be directly attributed to the PDMS used for the expandable matrix as well as the cover with the interconnected reservoirs. Since liquid absorption has to be considered beside liquid evaporation, it is not sufficient to coat the device only with a barrier material such as parylene-C. Consequently, all PDMS in direct contact with the liquid must be replaced with alternative materials featuring enhanced barrier properties. For instance, the cover with the reservoirs can be fabricated from a rigid polymer and be sealed on the bottom side with an elastic barrier membrane. In this case, the liquid is stored in a self-contained structure and the microheater PCB with the Expancel[®]-PDMS composite can still serve as the actuator.

Having addressed the aspect of storage stability, the concept of the *NeuroMedicator* can be further developed towards a stand-alone drug delivery system with wireless control. This would eliminate the need for any wire connection to the device after filling and implantation. Such a system is especially advantageous during behavioral experiments with small animals in neuroscience.

Acknowledgments

This work was performed in the frame of the Information Society Technologies (IST) Integrated Project *NeuroProbes* of the 6th Framework Program (FP6) of the European Commission (project no IST-027017). The authors acknowledge the support from Karsten Seidl, Patrick Ruther, Claas Müller, and the cleanroom facility of IMTEK, University of Freiburg as well as the support from Roland Gronmaier, Herbert Straatman and the cleanroom and machine shop facilities at HSG-IMIT. Furthermore, the authors would like to thank Björn Samel and Göran Stemme of Royal Institute of Technology Stockholm for useful discussions and insights. The provision of microspheres from Expancel, Sundsvall, Sweden, is gratefully acknowledged.

References

- [1] Lalley P M 1999 Microiontophoresis and pressure ejection *Modern Techniques in Neuroscience Research* ed U Windhorst and H Johansson (Berlin: Springer) chapter 7 pp 193–212
- [2] Lacey G 1997 Microelectrophoresis and pressure ejection methods *Neuroscience Methods: A Guide for Advanced Students* ed R Martin (Amsterdam: Harwood Academic Publishers) chapter 12 pp 80–4

- [3] Chen J, Wise K D, Hetke J F and Bledsoe S C Jr 1997 A multichannel neural probe for selective chemical delivery at the cellular level *IEEE Trans. Biomed. Eng.* **44** 760–9
- [4] Rathnasingham R, Kipke D R, Bledsoe S C Jr and McLaren J D 2004 Characterization of implantable microfabricated fluid delivery devices *IEEE Trans. Biomed. Eng.* **51** 138–45
- [5] Retterer S T, Smith K L, Bjornsson C S, Neeves K B, Spence A J H, Turner J N, Shain W and Isaacson M S 2004 Model neural prostheses with integrated microfluidics: a potential intervention strategy for controlling reactive cell and tissue responses *IEEE Trans. Biomed. Eng.* **51** 2063–73
- [6] Neeves K B, Lo C T, Foley C P, Saltzman W and Olbricht W L 2006 Fabrication and characterization of microfluidic probes for convection enhanced drug delivery *J. Controlled Release* **111** 252–62
- [7] Papageorgiou D P, Shore S E, Bledsoe S C and Wise K D 2006 A shuttered neural probe with on-chip flowmeters for chronic *in vivo* drug delivery *J. Microelectromech. Syst.* **15** 1025–33
- [8] Kanno S, Kobayashi R, Sanghoon L, Jicheol B, Fukushima T, Sakamoto K, Katayama N, Mushiake H, Tanaka T and Koyanagi M 2009 Development of Si neural probe with microfluidic channel fabricated using wafer direct bonding *Japan. J. Appl. Phys.* **48** 04C189-1–4
- [9] Seidl K, Spieth S, Herwik S, Steigert J, Zengerle R, Paul O and Ruther P 2010 In-plane silicon probes for simultaneous neural recording and drug delivery *J. Micromech. Microeng.* **20** 105006
- [10] Vrouwe E, Kelderman A and Blom M 2008 Microfluidic glass needle arrays for drug dosing during neural recording *Proc. 12th Int. Conf. on Miniaturized Systems for Chemistry and Life Sciences (μ TAS) (San Diego, CA, USA, 2008)* pp 378–80 (available at http://www.rsc.org/binaries/LOC/2008/PDFs/Papers/127_0337.pdf)
- [11] Pellinen D S, Moon T, Vetter R J, Miriani R and Kipke D R 2005 Multifunctional flexible parylene-based intracortical microelectrodes *Proc. 27th Annu. Int. Conf. of the IEEE EMBS (Shanghai, China, 2005)* pp 5272–5
- [12] Takeuchi S, Ziegler D, Yoshida Y, Mabuchi K and Suzuki T 2005 Parylene flexible neural probes integrated with microfluidic channels *Lab Chip* **5** 519–23
- [13] Ziegler D, Suzuki T and Takeuchi S 2006 Fabrication of flexible neural probes with built-in microfluidic channels by thermal bonding of parylene *J. Microelectromech. Syst.* **15** 1477–82
- [14] Metz S, Bertsch A, Bertrand D and Renaud P 2004 Flexible polyimide probes with microelectrodes and embedded microfluidic channels for simultaneous drug delivery and multi-channel monitoring of bioelectric activity *Biosens. Bioelectron.* **19** 1309–18
- [15] Fernández L J, Altuna A, Tijero M, Gabriel G, Villa R, Rodríguez M J, Batlle M, Vilares R, Berganzo J and Blanco F J 2009 Study of functional viability of SU-8-based microneedles for neural applications *J. Micromech. Microeng.* **19** 025007
- [16] Hochberg L R, Serruya M D, Friehs G M, Mukand J A, Saleh M, Caplan A H, Branner A, Chen D, Penn R D and Donoghue J P 2006 Neuronal ensemble control of prosthetic devices by a human with tetraplegia *Nature* **442** 164–71
- [17] Spieth S, Schumacher A, Seidl K, Hiltmann K, Haeberle S, McNamara R, Dalley J W, Edgley S A, Ruther P and Zengerle R 2009 Robust microprobe systems for simultaneous neural recording and drug delivery *Proc. 4th Eur. Conf. of the IFMBE (Antwerp, Belgium, 2008)* vol 22 ed J Vander Sloten *et al* (Berlin: Springer) pp 2426–30
- [18] Rohatgi P, Langhals N B, Kipke D R and Patil P G 2009 *In vivo* performance of a microelectrode neural probe with integrated drug delivery *Neurosurg. Focus* **27** E8
- [19] Criswell H E 1977 A simple chronic microinjection system for use with chemitrodes *Pharmacol. Biochem. Behav.* **6** 237–8
- [20] Bozarth M A and Wise R A 1980 Electrolytic microinfusion transducer system: an alternative method of intracranial drug application *J. Neurosci. Methods* **2** 273–5
- [21] Ikemoto S and Sharpe L G 2001 A head-attachable device for injecting nanoliter volumes of drug solutions into brain sites of freely moving rats *J. Neurosci. Methods* **110** 135–40
- [22] iPRECIO[®] Micro Infusion Pump (Tokyo, Japan: Primetech Corporation) www.iprecio.com (accessed 19/12/2011)
- [23] ithetis[™] Implantable Drug Delivery Device (Lausanne, Switzerland: Antlia SA) www.ithetis.com (accessed 19/12/2011)
- [24] ALZET Brain Infusion Kit (Cupertino, CA, USA: DURECT Corporation) www.alzet.com/products/brain_infusion_kit (accessed 19/12/2011)
- [25] Huang W 2002 On the selection of shape memory alloys for actuators *Mater. Des.* **23** 11–9
- [26] Gall K, Kreiner P, Turner D and Hulse M 2004 Shape-memory polymers for microelectromechanical systems *J. Microelectromech. Syst.* **13** 472–83
- [27] Ruhhammer J, Huesgen T and Woias P 2009 Bistable switching with a thermoelectrically driven thermopneumatic actuator *Proc. 15th Int. Conf. on Solid-State Sensors, Actuators and Microsystems (Transducers) (Denver, CO, USA, 2009)* pp 33–6
- [28] Janocha H 1988 Neue Aktoren *Proc. Int. Technology-Transfer Conf. Actuator (Actuator) (Bremen, Germany, 1988)* p 389
- [29] Kempe W and Schapper W 1990 Electrochemical actuators *Proc. Int. Conf. on New Actuators (Actuator) (Bremen, Germany, 1990)* p 162
- [30] Weng K Y 2001 Thermolysis reaction actuating pumps, TRAP *Proc. 5th Int. Conf. on Miniaturized Chemical and Biochemical Analysis Systems (μ TAS) (Monterey, CA, USA, 2001)* pp 409–10
- [31] Hong C C, Murugesan S, Kim S, Beaucage G, Choi J W and Ahn C H 2003 A functional on-chip pressure generator using solid chemical propellant for disposable lab-on-a-chip *Lab Chip* **3** 281–6
- [32] Han J, Lee S and Ahn C H 2006 A disposable on-chip pressure actuator using IR-induced thermolysis for sample transport *Proc. 10th Int. Conf. on Miniaturized Systems for Chemistry and Life Sciences (μ TAS) (Tokyo, Japan, 2006)* pp 588–90
- [33] Rossi C and Estève D 2005 Micropyrotechnics, a new technology for making energetic microsystems: review and prospective *Sensors Actuators A* **120** 297–310
- [34] Briand D, Dubois P, Bonjour L E, Guillot L and Bley U 2008 Large deformation balloon micro-actuator based on pyrotechnics on chip *Proc. 21st IEEE Int. Conf. on MEMS (Tucson, AZ, USA, 2008)* pp 535–8
- [35] Choi Y H, Son S U and Lee S S 2004 A micropump operating with chemically produced oxygen gas *Sensors Actuators A* **111** 8–13
- [36] Takashima A, Fukuda J and Suzuki H 2009 Chemically actuated microinjectors and programming with a microfluidic network *Proc. 15th Int. Conf. on Solid-State Sensors, Actuators and Microsystems (Transducers) (Denver, CO, USA, 2009)* pp 2282–5
- [37] Hong C C, Choi J W and Ahn C H 2007 An on-chip air-bursting detonator for driving fluids on disposable lab-on-a-chip systems *J. Micromech. Microeng.* **17** 410–7
- [38] Dominghaus H, Elsner P, Eyerer P and Hirth T 2008 *Kunststoffe: Eigenschaften und Anwendungen* 7th edn (Berlin, Germany: Springer)
- [39] Griss P, Andersson H and Stemme G 2002 Expandable microspheres for the handling of liquids *Lab Chip* **2** 117–20

- [40] Roxhed N, Rydholm S, Samel B, van der Wijngaart W, Griss P and Stemme G 2006 A compact, low-cost microliter-range liquid dispenser based on expandable microspheres *J. Micromech. Microeng.* **16** 2740–6
- [41] Samel B, Griss P and Stemme G 2007 A thermally responsive PDMS composite and its microfluidic applications *J. Microelectromech. Syst.* **16** 50–7
- [42] Samel B, Nock V, Russom A, Griss P and Stemme G 2007 A disposable lab-on-a-chip platform with embedded fluid actuators for active nanoliter liquid handling *Biomed. Microdevices* **9** 61–7
- [43] Samel B, Chretien J, Yue R, Griss P and Stemme G 2007 Wafer-level process for single-use buckling-film microliter-range pumps *J. Microelectromech. Syst.* **16** 795–801
- [44] Spieth S, Schumacher A, Kallenbach C, Messner S and Zengerle R 2010 NeuroMedicator—a disposable drug delivery system with silicon microprobes for neural research *Proc. 23rd IEEE Int. Conf. on MEMS (Hong Kong, 2010)* pp 983–6
- [45] Neves H P, Orban G A, Koudelka-Hep M and Ruther P 2007 Development of modular multifunctional probe arrays for cerebral applications *Proc. 3rd Int. IEEE EMBS Conf. on Neural Eng. (Kohala Coast, HI, USA, 2007)* pp 104–9
- [46] Ruther P *et al* 2008 The NeuroProbes project—multifunctional probe arrays for neural recording and stimulation *Biomed. Tech.* **53** 238–40
- [47] Rice M E, Gerhardt G A, Hierl P M, Nagy G and Adams R N 1985 Diffusion coefficients of neurotransmitters and their metabolites in brain extracellular fluid space *Neuroscience* **15** 891–902
- [48] Product Specification 2006 *EXPANCEL DU, Dry Unexpanded Microspheres* (Sundsvall, Sweden: Expancel) 2006.01
- [49] Baehr H D and Stephan K 2006 *Wärme- und Stoffübertragung* 5th edn (Berlin: Springer)
- [50] Incropera F, DeWitt D, Bergman T and Lavine A 2007 *Fundamentals of Heat and Mass Transfer* 6th edn (Hoboken, NJ: Wiley)
- [51] Lee S and Lee S S 2008 Shrinkage ratio of PDMS and its alignment method for the wafer level process *Microsyst. Technol.* **14** 205–8
- [52] Grand L *et al* 2010 Short and long term biocompatibility of NeuroProbes silicon probes *J. Neurosci. Methods* **189** 216–29